

Mean Surface Stress Curl over the Oceans as Determined from the Vorticity Budget of the Atmosphere

E. O. HOLOPAINEN¹

Geophysical Fluid Dynamics Program, Princeton University, Princeton, NJ 08540

A. H. OORT

Geophysical Fluid Dynamics Laboratory/NOAA, Princeton University, Princeton, NJ 08540

(Manuscript received 4 March 1980, in final form 9 October 1980)

ABSTRACT

The vertically integrated atmospheric vorticity budget over the oceans offers, in principle, a possibility of determining the surface stress curl from upper wind data without the need to specify a relationship between the surface stress and surface wind. Results for the wind stress curl obtained by this vorticity method, using upper wind data for the period 1968–73, are compared with the recent stress-curl calculations by Hellerman from surface data.

The two completely independent methods give basically similar mean latitudinal distributions of the stress curl. In the midlatitudes of the Southern Hemisphere, where the transient eddies are the main mechanism of vorticity transfer, the two estimates of the basin-wide longitudinal averages of the stress curl do not deviate from each other by $\geq 20\%$. However, in the Northern Hemisphere the agreement is less. This seemingly strange result appears to be due to the sensitivity of the vorticity method to errors in the estimates of vorticity advection by the standing waves.

It is concluded that for the time being the geographical pattern of the mean surface stress curl can, at least in the Northern Hemisphere, be estimated from surface data (using a drag formulation) more accurately than from upper wind data (using the vorticity method). Together the two methods offer a useful quality check for the upper air data.

1. Introduction

The curl of surface wind stress (curl τ_s) is a quantity of paramount importance in studies of the oceanic large-scale circulation. The climatological distribution of this quantity is normally obtained by evaluating the stress from surface observations with the aid of a drag-law formulation (e.g., Hellerman, 1967). However, considerable difficulties are involved in applying this method. Besides problems in formulating the dependence of the drag coefficient on stability and wind conditions, the inadequate geographical coverage of surface data also poses a serious problem. Naturally, the relative uncertainty associated with estimates of the curl of wind stress is larger than the uncertainty in the stress itself. For these reasons, it would be of great value to get estimates of curl τ_s by independent means.

The vorticity budget of the atmosphere offers, in principle, an opportunity to determine curl τ_s from upper wind data alone, as was first pointed out in

1956 by Mintz.² Later this was used by one of the present authors (Holopainen, 1967) to calculate curl τ_s (and the associated Sverdrup transports) for the oceans in the Northern Hemisphere north of $\sim 20^\circ\text{N}$, by using upper wind statistics compiled by Crutcher (1959). The results were encouraging. For example, the values obtained by the vorticity method for the annual-mean Sverdrup circulation in the Gulf Stream and Kuroshio were rather realistic.

In this paper we report determinations of curl τ_s by the vorticity method using global upper air statistics for the 5-year period 1968–73. A description of the method and the data used is given in Section 2. The presentation of the results (Section 3) is followed by an analysis of the uncertainties associated with the vorticity method (Section 4) and a discussion of its possible future applications (Section 5).

¹ On leave from the Department of Meteorology, University of Helsinki, Helsinki, Finland.

² Mintz, Y., 1956: An empirical determination of surface drag coefficients for extended-range and long-range numerical weather forecasting and the study of the general circulation (Preliminary Report). Sci. Rep. No. 3, Contract AF 19(604)-1286, Department of Meteorology, University of California, Los Angeles.

2. Method and the data

The equations of horizontal motion, averaged with respect to time, can be written in a spherical (λ, ϕ, p) coordinate system as (Holopainen, 1978)

$$\frac{\partial \bar{\mathbf{V}}}{\partial t} = -\bar{\mathbf{V}} \cdot \nabla \bar{\mathbf{V}} - \bar{\omega} \frac{\partial \bar{\mathbf{V}}}{\partial p} - \nabla \bar{\Phi} - f \mathbf{k} \times \bar{\mathbf{V}} + \mathbf{A}_H + \mathbf{A}_V + \mathbf{F}_H + \mathbf{F}_V, \quad (1)$$

where

$$\begin{aligned} \mathbf{A}_H &= A_\lambda \mathbf{i} + A_\phi \mathbf{j}, \quad (2) \\ A_\lambda &= -\frac{1}{a \cos \phi} \frac{\partial}{\partial \lambda} \overline{u'u'} \\ &\quad - \frac{1}{a \cos \phi} \frac{\partial}{\partial \phi} \overline{u'v'} \cos \phi + \frac{\overline{u'u'}}{a} \tan \phi, \\ A_\phi &= -\frac{1}{a \cos \phi} \frac{\partial}{\partial \lambda} \overline{u'v'} \\ &\quad - \frac{1}{a \cos \phi} \frac{\partial}{\partial \phi} \overline{v'v'} \cos \phi - \frac{\overline{u'u'}}{a} \tan \phi \\ \mathbf{A}_V &= -\frac{\partial}{\partial p} \overline{\mathbf{V}'\omega'}. \quad (3) \end{aligned}$$

In these equations λ is longitude, ϕ latitude, p pressure, \mathbf{V} ($=u\mathbf{i} + v\mathbf{j}$) the horizontal velocity vector, $\omega = dp/dt$, and Φ the geopotential height. Further, ∇ is the horizontal del operator, \mathbf{k} the unit vector in the vertical, a the mean radius of the earth, and f the Coriolis parameter. The bar denotes a time-average and a prime a deviation from it. \mathbf{A}_H and \mathbf{A}_V are forces acting on the time-mean flow due to the presence of large-scale turbulence (synoptic disturbances). These forces in principle can be described in terms of large-scale quantities. \mathbf{F}_H and \mathbf{F}_V (which we do not have any direct data about) are the frictional forces acting on the time-mean flow due to mesoscale and small-scale turbulence; $\mathbf{F} = \mathbf{F}_H + \mathbf{F}_V$ is the frictional force normally used in studies of atmospheric large-scale flow. These definitions of \mathbf{A} and \mathbf{F} involve a scale separation, in which the separation point is related to the interval between the upper wind observations (12 h). An important point is that close to the ocean surface the vertical eddy stresses (which cause \mathbf{F}_V) are only due to small-scale turbulence, and that relatively well-established schemes exist for their parameterization in terms of the large-scale flow.

Taking the curl of (1) gives the vorticity equation of the time-averaged flow

$$\begin{aligned} \frac{\partial \bar{\zeta}}{\partial t} &= -\bar{\mathbf{V}} \cdot \nabla \bar{\eta} - \bar{\eta} \nabla \cdot \bar{\mathbf{V}} + \text{curl } \mathbf{A}_H + \text{curl } \mathbf{A}_V \\ &\quad - \left(\bar{\omega} \frac{\partial \bar{\zeta}}{\partial p} + \mathbf{k} \cdot \nabla \bar{\omega} \times \frac{\partial \bar{\mathbf{V}}}{\partial p} \right) + \text{curl } \mathbf{F}, \quad (4) \end{aligned}$$

where $\text{curl } \mathbf{B} = \mathbf{k} \cdot \nabla \times \mathbf{B}$ (\mathbf{B} an arbitrary vector field), $\zeta = \text{curl } \mathbf{V}$ and $\eta = \zeta + f$. This equation can also be obtained by time-averaging the vorticity equation. In that case one finds that

$$\begin{aligned} \text{curl } \mathbf{A}_H + \text{curl } \mathbf{A}_V &= -\nabla \cdot \overline{\zeta' \mathbf{V}'} - \overline{\omega' \frac{\partial \zeta'}{\partial p}} - \mathbf{k} \cdot \nabla \overline{\omega'} \times \frac{\partial \overline{\mathbf{V}'}}{\partial p}. \quad (5) \end{aligned}$$

We now take into account that \mathbf{F}_V can be represented in terms of the vertical eddy stress τ (acting on a horizontal surface), i.e.,

$$\mathbf{F}_V = -g \frac{\partial \tau}{\partial p}, \quad (6)$$

and that for long-term average conditions the left-hand side of (4) becomes very small. Then, by integrating (4) with respect to pressure and using the boundary conditions

$$\begin{aligned} \bar{\omega} &= 0, \quad \overline{\mathbf{V}'\omega'} = 0, \quad \tau = 0 \\ &\quad \text{at } p = 0 \text{ (top of the atmosphere),} \\ \bar{\omega} &= 0, \quad \overline{\mathbf{V}'\omega'} = 0, \quad \tau = \tau_s \\ &\quad \text{at } p = p_0 \text{ (ocean surface),} \end{aligned}$$

we obtain

$$\begin{aligned} \text{curl } \bar{\tau}_s &= -\int_0^{p_0} \bar{\mathbf{V}} \cdot \nabla \bar{\eta} \frac{dp}{g} + \int_0^{p_0} \text{curl } \mathbf{A}_H \frac{dp}{g} \\ &\quad - \left[\int_0^{p_0} \bar{\zeta} \nabla \cdot \bar{\mathbf{V}} \frac{dp}{g} + \int_0^{p_0} \bar{\omega} \frac{\partial \bar{\zeta}}{\partial p} \frac{dp}{g} \right. \\ &\quad \left. + \int_0^{p_0} \left(\mathbf{k} \cdot \nabla \bar{\omega} \times \frac{\partial \bar{\mathbf{V}}}{\partial p} \right) \frac{dp}{g} - \int_0^{p_0} \text{curl } \mathbf{F}_H \frac{dp}{g} \right]. \quad (7) \end{aligned}$$

It will be shown in Section 4 that the terms in brackets make only minor contributions compared with the first two terms on the right-hand side of (7). Therefore, the basic equation for the vorticity method is

$$\boxed{\text{curl } \bar{\tau}_s = M + T}, \quad (8)$$

where

$$M = M_1 + M_2, \quad (9)$$

$$M_1 = -\int_0^{p_0} \bar{\mathbf{V}} \cdot \nabla \bar{\zeta} \frac{dp}{g}, \quad (10)$$

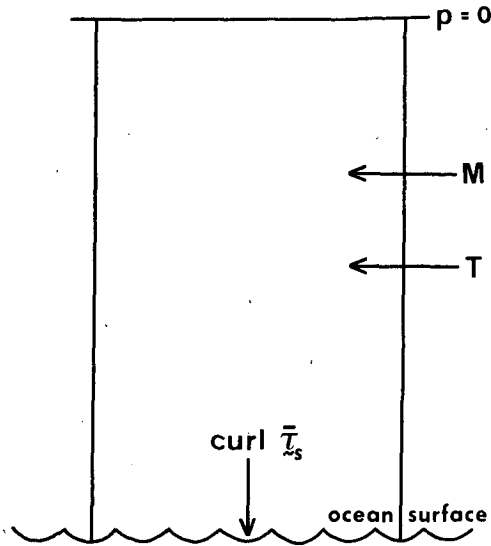


FIG. 1. Scheme of the time-mean vertically integrated budget of vorticity in an atmospheric column extending from the surface of the ocean to the top of the atmosphere [see Eq. (8)].

$$M_2 = - \int_0^{p_0} \beta \bar{v} \frac{dp}{g}, \quad (11)$$

$$T = \int_0^{p_0} \text{curl } \mathbf{A}_H \frac{dp}{g}. \quad (12)$$

The terms M and T are approximately equal to the vorticity flux convergence into the air column by

the time-mean motion and the transient fluctuations, respectively.

In light of (8), $\text{curl } \bar{\tau}_s$ represents the only source or sink of vorticity for the atmospheric column extending from the top of the atmosphere down to the ocean surface (Fig. 1). (At any particular level the stretching or contraction of vortex tubes, represented by the term $-\bar{\eta} \nabla \cdot \bar{\mathbf{V}} \approx -f \nabla \cdot \bar{\mathbf{V}}$, is an important source or sink. However, when integrated over the entire air column this term disappears.) For example, in the North Pacific low in winter, $\text{curl } \bar{\tau}_s$ is definitely positive and the atmospheric column loses vorticity to the ocean. In the mean, this loss has to be counterbalanced by the net horizontal inflow either in the form of M or T or both. Because the vorticity fluxes have their largest amplitude in the upper troposphere and lower stratosphere, $\text{curl } \bar{\tau}_s$ is, through (8), determined by (and calculable in terms of) the upper level winds.

The basic data used here for the evaluation of M and T are the worldwide aerological observations made during May 1968–April 1973 (see Fig. 2). They are part of a 15-year data set compiled and processed at the Geophysical Fluid Dynamics Laboratory³ using the method described in Oort and Rasmusson (1971). Analyses of the various basic quantities were made for each month of the 5-year period. To obtain the annual and seasonal statistics used here the in-

³ Oort, A. H., 1981: Global atmospheric circulation statistics, 1958–1973. NOAA Prof. Pap. (in preparation).

DISTRIBUTION WIND REPORTING STATIONS FOR JAN 71 AT 300mb (N_{GLOBE} = 735)

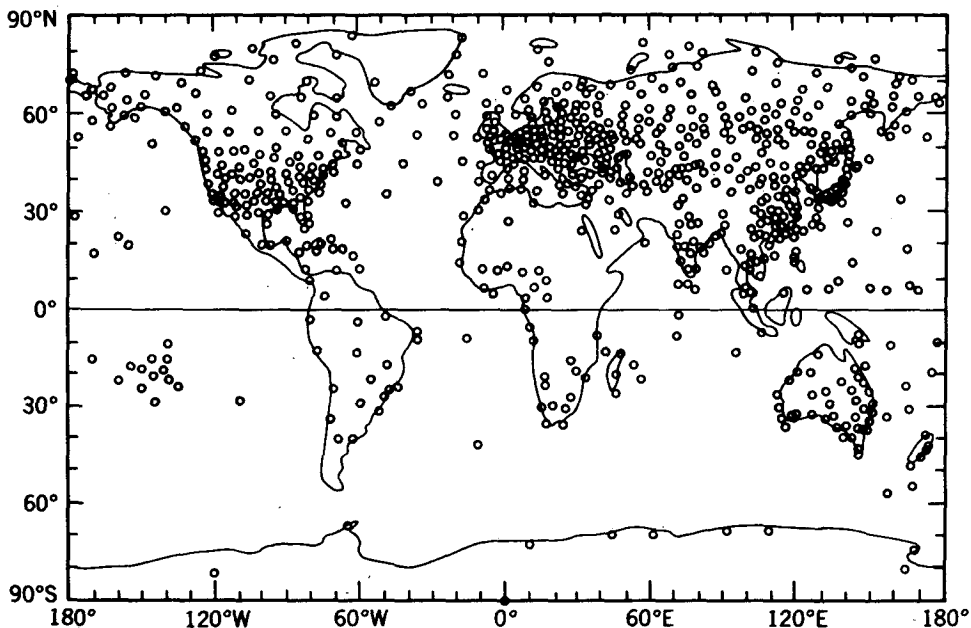


FIG. 2. Distribution of the rawinsonde stations, from which the basic observations for the GFDL data set were obtained at 300 mb for a typical month (January 1971).

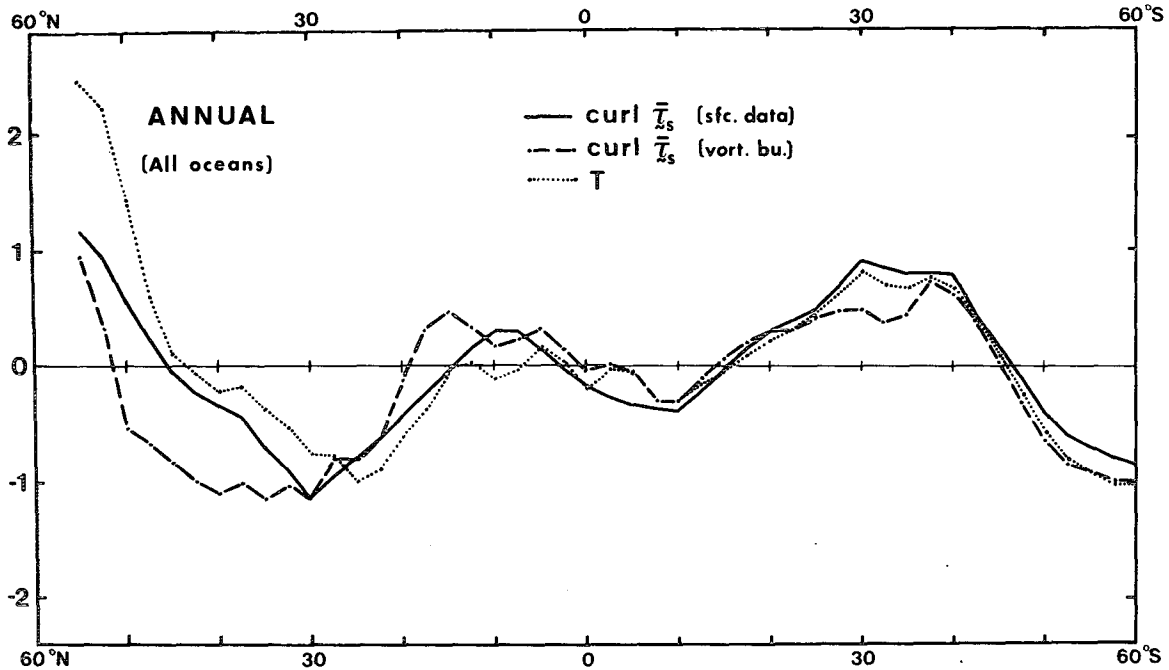


FIG. 3. Annual-mean distribution of $\text{curl } \bar{\tau}_s$ (sfc data), $\text{curl } \bar{\tau}_s$ (vort bu) and T averaged longitudinally over all oceans. The curve for $\text{curl } \bar{\tau}_s$ (sfc data) is derived from the new calculations made by Hellerman (personal communication) on the basis of surface data. Units: 10^{-7} N m^{-3} .

dividual monthly analyses were combined to evaluate 5-year mean and eddy statistics.

The quantities needed in our calculations are the 2-dimensional fields of \bar{u} , \bar{v} , $\overline{u'u'}$, $\overline{u'v'}$, $\overline{v'v'}$ for different pressure levels. The levels used in the calculations are 50, 100, 200, 300, 400, 500, 700, 850, 900, 950 and 1000 mb. In the horizontal plane a 73×73 grid with $\Delta\lambda = 5^\circ$ and $\Delta\phi = 2.5^\circ$ was used. This data set will be referred to in the following as the GFDL data.

One question related to the upper wind data is that in their original form they do not exactly satisfy the requirement of zero mean mass flux across a latitude circle. This requirement implies that

$$\int_0^{2\pi} M_2 d\lambda = 0. \tag{13}$$

An additive correction (constant at each latitude) was applied to the local estimates of M_2 assuming that all spurious contributions come only from the ocean areas, where the upper wind data are sparse, and that values of \bar{v} (and M_2) are correct over the continents, where the network of upper wind stations is much more satisfactory. The geographical variation of the mean surface pressure related to mountains was taken into account in this correction. In this way M_{corr} was obtained. In the Northern Hemisphere this correction made an insignificant contribution, but in the Southern Hemisphere it was more important.

Thus, the actual formula of the "vorticity budget

(vort bu) method" used was

$$\text{curl } \bar{\tau}_s \text{ (vort bu)} = M_{\text{corr}} + T \tag{14}$$

The values of $\text{curl } \bar{\tau}_s$ (vort bu) will be compared with those obtained by Hellerman (personal communication) from surface data with the aid of the bulk aerodynamic formula

$$\text{curl } \bar{\tau}_s \text{ (sfc data)} = \text{curl } \rho C_D |\bar{\mathbf{V}}_s| \bar{\mathbf{V}}_s, \tag{15}$$

where ρ is the air density, C_D the drag coefficient and \mathbf{V}_s the wind at anemometer level. The procedure of calculating $\bar{\tau}_s$ (sfc data) was similar to the one used by Hellerman (1967). However, differences are that in the present calculations a large collection of synoptic observations was used instead of monthly wind-rose data, and that a new drag formulation by Bunker (1976) was used for C_D .

The estimates of $\text{curl } \bar{\tau}_s$ (vort bu) and $\text{curl } \bar{\tau}_s$ (sfc data) are both indirect estimates of the true $\text{curl } \bar{\tau}_s$. In principle, they should be equal if the assumptions made in deriving (14) and (15) were correct, and if upper air and surface data were adequate for getting reliable estimates of the right-hand sides of (14) and (15), respectively.

3. Results

Fig. 3 shows for the annual-mean conditions the meridional distribution of $\text{curl } \bar{\tau}_s$ (sfc data) and $\text{curl } \bar{\tau}_s$ (vort bu).

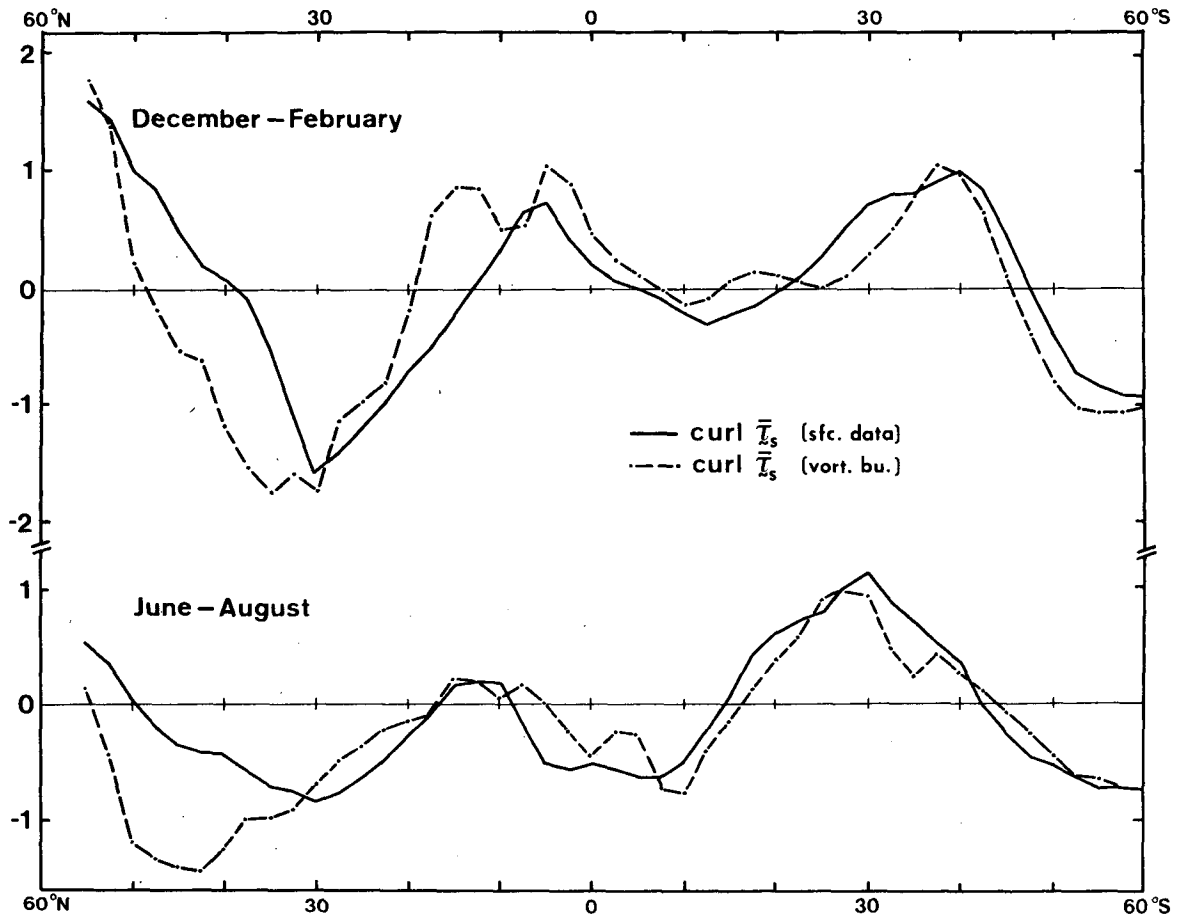


FIG. 4. Distribution of $\text{curl } \bar{\tau}_s$ (sfc data) and $\text{curl } \bar{\tau}_s$ (vort bu), averaged longitudinally over all oceans, for December-February (upper part) and June-August (lower part). Units: 10^{-7} N m^{-3} .

$\bar{\tau}_s$ (vort bu) averaged at each latitude longitudinally over the whole oceanic domain. For reasons which will become obvious later, the full geographical distribution of $\text{curl } \bar{\tau}_s$ (vort bu) will not be discussed.

A fair amount of agreement, with respect to both amplitude and phase of the meridional variation, is found between the independent estimates of $\text{curl } \bar{\tau}_s$ (sfc data) and $\text{curl } \bar{\tau}_s$ (vort bu). It is at first sight surprising that the agreement is best in the Southern Hemisphere, where the amount of both surface and upper air data is smallest. South of 35°S the two estimates agree within $\sim 20\%$.

Fig. 4 shows the results for $\text{curl } \bar{\tau}_s$ (sfc data) and $\text{curl } \bar{\tau}_s$ (vort bu) for December-February and June-August. Essentially the same features as in Fig. 3 (surprisingly good agreement in the Southern Hemisphere not so good agreement in the Northern Hemisphere) can be seen also in the results for the extreme seasons.

A possible explanation of the above features is, as will be shown in more detail in the next section, that the vorticity method may produce spurious features in those areas (like the entire Northern Hemi-

sphere) where the time-mean atmospheric circulation contains sizeable contributions from the so-called stationary disturbances. The time-mean circulation in the Southern Hemisphere is much more zonally symmetric than that in the Northern Hemisphere. Therefore the essential features of the vorticity budget (such as the meridional profile of $\overline{u'v'}$ are in the Southern Hemisphere perhaps already satisfactorily described with the aid of the few available stations (see Fig. 2).

4. Shortcomings of the vorticity method

Errors arise in the calculations of $\text{curl } \bar{\tau}_s$ (vort bu) due to (i) neglecting the terms in brackets in Eq. (7), (ii) systematic biases in the estimates of M and T due to deficiencies in the upper-wind statistics.

Considering first (i), order of magnitude estimates of the first three terms were made using the observed values of $\nabla \cdot \bar{\mathbf{V}}$ (which undoubtedly have large errors) and the values of $\bar{\omega}$ obtained from $\nabla \cdot \bar{\mathbf{V}}$ through the continuity equation ($\nabla \cdot \bar{\mathbf{V}} + \partial \bar{\omega} / \partial p = 0$). It was found that they are typically one order of magnitude

smaller than M and T . It seems also reasonable to assume that in the large-scale averages considered here the relative contribution of $\text{curl } F_H$ in (7) is negligible. In other words, the role of horizontal momentum fluxes associated with the small-scale and mesoscale eddies is small compared with that due to the large-scale eddies. The relative error in $\text{curl } \tau_s$ (vort bu) due to (i) is perhaps only of the order of 10%.

Going now to point (ii) one tends automatically to think that in the Northern Hemisphere, due to differences in the amount of data available, the errors in the estimates of M and T would be smaller than in the Southern Hemisphere. However, this may not be the case for the following reasons.

One basic difference between the atmospheric general circulation in the two hemispheres is that the so-called stationary disturbances (or standing waves), caused by large mountain barriers and the land/ocean thermal contrasts, have a much larger amplitude in the Northern than in the Southern Hemisphere. The term M is essentially the local vorticity advection in standing waves and consists [see Eqs. (10)–(11)] of two terms, M_1 and M_2 (advection of the mean relative vorticity and earth's vorticity, respectively), which are individually large by magnitude but of opposite sign. This is shown clearly in Fig. 5, which gives the latitudinal profiles of M_1 and M_2 over the Northern Hemisphere oceans in winter, when the stationary disturbances have their largest amplitude. Thus, small relative errors in the estimates of M_1 and M_2 may cause large relative errors in their sum M . The major difficulty probably lies in the determination of the advection of the mean relative vorticity M_1 which at the present time cannot be evaluated accurately enough from the available data. Comparing our present results with the corresponding quantities involved in Holopainen (1967, 1978), it appears that uncertainties as large as $1 \times 10^{-7} \text{ N m}^{-3}$ are associated with the estimates of $\text{curl } \tau_s$ (vort bu) in the extratropical latitudes of the Northern Hemisphere. The results shown in Figs. 3 and 4 become more understandable when they are considered with this uncertainty in mind.

The term T [see Eq. (12)] is determined by the anisotropic part ($\overline{u'v'}$, $\overline{u'u'} - \overline{v'v'}$) of the atmospheric large-scale turbulence (Holopainen, 1978). In the longitudinal, basin-wide averages shown here, T is essentially determined by the second derivative of $\overline{u'v'}$ with respect to latitude. Therefore, the estimates of T are also rather sensitive to possible biases in the basic data. Quantitative error limits are difficult to establish. Qualitatively, however, the relative errors in M are, due to the counterbalancing mentioned above, probably larger than those in T . From Fig. 3 it is interesting to note that the latitudinal profile of $\text{curl } \tau_s$ (sfc data) correlates better with T than with $M_{\text{corr}} + T$. This is another indication that

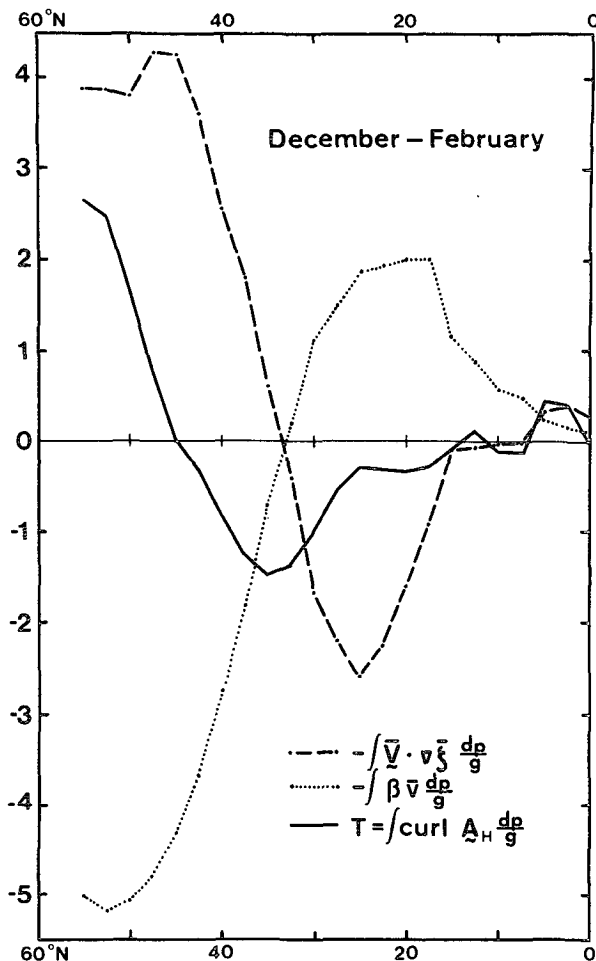


FIG. 5. Latitudinal distribution of the terms $-\bar{v} \cdot \nabla \bar{\xi}$, $-\beta \bar{v}$ and $\text{curl } A_H$ integrated vertically over the depth of the atmosphere and averaged longitudinally over the oceanic regions for the Northern Hemisphere in December–February. Units: 10^{-7} N m^{-3} .

although a mass balance correction (which affects only M_2) is made, the errors made in estimating M tend to produce spurious features in the pattern of $\text{curl } \tau_s$ (vort bu). This result is compatible with the findings of Mak (1978). He demonstrated that in the Northern Hemisphere large uncertainties exist concerning the zonally averaged meridional flux of zonal momentum in standing waves (which is related to the zonally averaged value of M_1). Over the oceanic sectors the errors in the estimates of M_1 (and thus also of M) are naturally larger than in the zonally averaged conditions.

The distribution of $\text{curl } \tau_s$ (vort bu) in winter was also calculated from a 10-year data set (Lau, 1978; referred to in the following as “NMC data”) based on the routine upper air numerical analyses of the U.S. National Meteorological Center. The 10 winters averaged in the NMC data set were those of 1965/66 through 1975/76, except the winter of 1969/70. Some

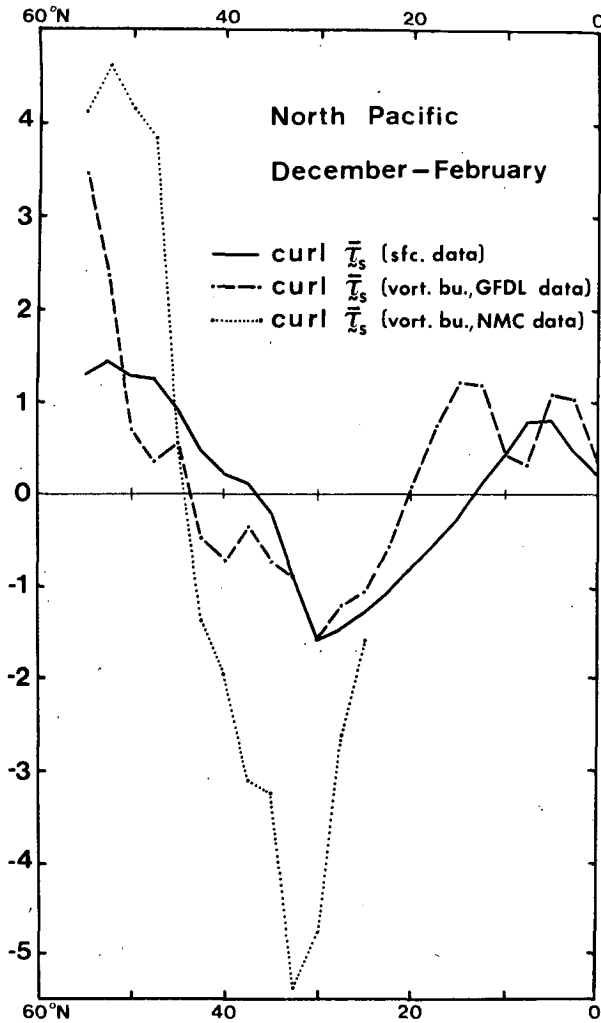


FIG. 6. Three estimates of $\text{curl } \bar{\tau}_s$, averaged longitudinally over the North Pacific region, in December-February. Units: 10^{-7} N m^{-3} . Shown are $\text{curl } \bar{\tau}_s$ (sfc data) as a continuous, $\text{curl } \bar{\tau}_s$ (vort bu, GFDL data) as a dashed and $\text{curl } \bar{\tau}_s$ (vort bu, NMC data) as a dotted line.

differences in the results may be expected due to the different time periods and different analysis procedures used in the GFDL and NMC upper air data sets, and in the surface data set. The longitudinally averaged values of $\text{curl } \bar{\tau}_s$ (vort bu, NMC data) are shown in Fig. 6 together with those of $\text{curl } \bar{\tau}_s$ (sfc data) and $\text{curl } \bar{\tau}_s$ (vort bu, GFDL data) for the area of the North Pacific, where there is a large hole in the network of aerological stations even in the Northern Hemisphere. One notices that, both in the regions of maximum anticyclonic stress ($\sim 30^\circ\text{N}$) and of maximum cyclonic stress ($\sim 50^\circ\text{N}$), $\text{curl } \bar{\tau}_s$ (vort bu, NMC data) is two to three times larger than $\text{curl } \bar{\tau}_s$ (sfc data) and $\text{curl } \bar{\tau}_s$ (vort bu, GFDL data), which show better mutual agreement. The reason for this large discrepancy is not known. One hypothesis is that the NMC data over the North Pacific have a

small systematic bias (e.g., due to the use of forecasts as the first guess, which in the data-void region actually determines the final analysis). In delicate budgets, like the one for vorticity, such a bias may cause large spurious features. The discrepancy should not be interpreted to imply that the NMC analyses are, in general, worse than the GFDL analyses. A positive outcome from this comparison is that the atmospheric vorticity budget can perhaps be used in conjunction with the estimates of $\text{curl } \bar{\tau}_s$ (sfc data) as a method of quality control for upper wind data.

5. Discussion and conclusions

The vorticity method used here for the determination of $\text{curl } \bar{\tau}_s$ is analogous to the method of determining the total eastward torque (frictional torque + mountain torque) of the atmosphere on the earth from the vertically integrated, zonally averaged equation for zonal angular momentum. In this last equation the crucial term, the divergence of the meridional flux of zonal angular momentum, can be estimated fairly reliably from upper wind statistics (e.g., Oort and Bowman, 1974). The momentum method of determining the stress of the atmosphere on the earth can be used only in the zonally averaged conditions, for which the zonal pressure gradient term disappears in the free atmosphere. The difficulty of determining ageostrophic velocities accurately enough makes it almost impossible to apply this method in an arbitrary geographical location. The vorticity equation does not contain the sensitive balance between the pressure field and the wind field, and can in principle be applied over any area where upper wind data are available. However, as the results of this paper demonstrate, the vorticity budget contains another kind of sensitive balance, which makes its use difficult over those areas, where the time-mean atmospheric circulation contains a significant contribution from the standing waves.

The main conclusion from the present work is that for the time being the drag method, based on surface data, is probably still the best method of determining the geographical distribution of surface stress and related quantities. However, the vorticity method is an interesting alternative, which should be applied when new and hopefully better upper-wind data sets (like those from the FGGE experiment) become available. In fact, with improvement of satellite data (used in combination with surface pressure data as obtained from, e.g., buoys), the vorticity method may well become equal to or better (free of assumptions) than the drag method. If not for anything else, the vertically integrated atmospheric vorticity budget can in any case be used, together with the surface stress estimates obtained by the drag method, as one way of checking the upper wind data for possible biases.

Acknowledgments. The authors are grateful to Mr. Sol Hellerman for letting them use his new, unpublished estimates of the curl of the wind stress based on surface data, to Dr. N.-C. Lau for giving access to his (NMC) data set and for his cooperation in many ways, and to Dr. K. Bryan for his continuous interest in this work. This work was performed when one of the authors (EOH) was on a Visiting Scientist appointment in the Geophysical Fluid Dynamics Program, Princeton University, and was supported by NOAA Grant 04-7-022-44017.

REFERENCES

- Bunker, A. F., 1976: Computations of surface energy flux and annual air-sea interaction cycles of the North Atlantic Ocean. *Mon. Wea. Rev.*, **104**, 1122-1140.
- Crutcher, H., 1959: Upper wind statistics charts of the Northern Hemisphere. Vols. 1 and 2. NAVAER 50-1C-535, Office of the Chief of the U.S. Naval Operations, Washington, DC.
- Hellerman, S., 1967: An updated estimate of the wind stress on the world ocean. *Mon. Wea. Rev.*, **95**, 607-626.
- Holopainen, E. O., 1967: A determination of the wind-driven ocean circulation from the vorticity budget of the atmosphere. *Pure Appl. Geophys.*, **67**, 156-165.
- , 1978: On the dynamic forcing of the long-term mean flow by the large-scale Reynolds' stresses in the atmosphere. *J. Atmos. Sci.*, **35**, 1596-1604.
- Mak, M., 1978: On the observed momentum flux by standing waves. *J. Atmos. Sci.*, **35**, 340-346.
- Lau, N.-C., 1978: On the three-dimensional structure of the observed transient eddy statistics of the Northern Hemisphere wintertime circulation. *J. Atmos. Sci.*, **35**, 1900-1923.
- Oort, A. H., and H. D. Bowman II, 1974: A study of the mountain torque and its interannual variations in the Northern Hemisphere. *J. Atmos. Sci.*, **31**, 1974-1982.
- , and E. M. Rasmusson, 1971: *Atmospheric Circulation Statistics*. NOAA Prof. Pap. No. 5, 323 pp. [NTIS COM-72-50295].